

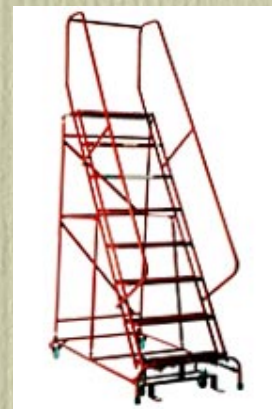
# Hybrid Mesons in the Flux Tube Model

---

- flux tubes
- hybrids
- checks:
  - comparison to lattice
  - adiabatic + small
  - oscillation
- IKP decay model
- extensions:
  - charge radii
  - surface mixing
  - spin dependence
  - spin dependence II
  - vector decay model
  - other applications
- conclusions



construct a ladder from the debris of nuclear  
explosions to the beauty of Babylon



PHYSICAL REVIEW B

VOLUME 47, NUMBER 6

1 FEBRUARY 1993-II

**Excitation spectrum of Heisenberg spin ladders**

T. Barnes

*Physics Division and Center for Computationally Intensive Physics, Oak Ridge National Laboratory, Oak Ridge, Tennessee 37831-6373  
and Department of Physics, University of Tennessee, Knoxville, Tennessee 37996-1200*

# Flux Tubes

## strong coupling Hamiltonian lattice gauge theory

$$H = \frac{g^2}{2a} \sum_i (E_i^+ E_{i+}) + \sum_\mu m_i c_i c_{i\mu} + \frac{1}{a} \sum_{\langle i,j \rangle} (c_i^\dagger \alpha_{ij} c_j^\dagger) u_i c_{i\mu} c_{j\mu} + \frac{1}{4g^2} \sum_p (\pi(N - U_p - U_p^\dagger))$$



## strong coupling Hamiltonian lattice gauge theory

$$H = \frac{g^2}{2a} \sum_i E_i^* E_{i+1} + \sum_\mu m_i c_i c_{i+\mu} + \frac{1}{a} \sum_{\langle i,j \rangle} C_i^\mu \alpha_{ij} U_\mu(u) c_{i+\mu} + \frac{1}{4g^2} \sum_p (\epsilon p N - U_p - C_p)$$



'topological' sector



## strong coupling Hamiltonian lattice gauge theory

$$H = \frac{g^2}{2a} \sum_i E_i^* E_{i+1} + \sum_i m_i c_i c_{i+1} + \frac{1}{a} \sum_{\langle i,j \rangle} C_i^* \alpha_{ij} C_j (a) c_{i+j, \mu} + \frac{1}{4g^2} \sum_p (\epsilon p N - U_p - C_p^*)$$



adiabatic  
 small oscillation  
 nonrelativistic beads  
 $m_b = b a$

# string Hamiltonian

$$H = h_0 R + \sum_n \left( \frac{p_n^2}{2 h_0} + \frac{\hbar}{2n} (y_n - y_{n+1})^2 \right)$$

$$s_{n\lambda}=\sum_n g_n(\lambda)\sqrt{\frac{2}{N+1}}\sin\frac{n\theta\ell\pi}{N+1}$$

$$g_n(\lambda)=\sum_n s_{n\lambda}\sqrt{\frac{2}{N+1}}\sin\frac{n\theta\ell\pi}{N+1}$$

$$H = h_0 R + \sum_{n\lambda} \left( \frac{p_n^2}{2 h_0} + \frac{h_0}{2} \omega_n^2 s_{n\lambda}^2 \right)$$

$$\omega_n = \frac{2}{n} \sin \frac{\pi n}{2(N+1)}$$

$$x_\ell = \frac{\pi}{R}$$

$$\alpha_{n\lambda}=\sqrt{\frac{h_0\omega_n}{2}}s_{n\lambda}+i\frac{p_{n\lambda}}{\sqrt{h_0\omega_n}}$$

$$H = h_0 R + \sum_{n\lambda} \omega_n \left( \alpha_{n\lambda}^\dagger \alpha_{n\lambda} + \frac{1}{2} \right)$$

$$H = h_0 R - \left( \frac{i}{\pi a^2} R - \frac{1}{4} - \frac{\pi}{(2R)} \right) + \sum_{n\lambda} \omega_n \alpha_{n\lambda}^\dagger \alpha_{n\lambda}$$

# Hybrids

# Hybrid State

$$LM_L(SM; \Lambda\{n_{\alpha_1}, n_{\alpha_2}\}) \propto \int d^3r_1 dr_2 P_{LM; \Lambda}^L(r) R_{1,2,s}^L r_{1,2,s} \prod_{\alpha} (\alpha'_{\alpha_1} / e^{i\omega_1 t} - \alpha'_{\alpha_2} / e^{i\omega_2 t} - i)$$

$$\Lambda = \sum_{\alpha} (n_{\alpha_1} - n_{\alpha_2})$$

$$E = E_0 + N \frac{\pi}{R}$$

$$N = \sum_{\alpha=1}^{\infty} (m n_{\alpha_1} + m_{\alpha_2})$$

# Hybrid Quantum Numbers

$$P(LM_L(SM_S; \Lambda\{n_{\alpha_1}, n_{\alpha_2}\})) = (-1)^{k+\Lambda} \times LM_L(SM_S; \Lambda\{n_{\alpha_1}, n_{\alpha_2}\})$$

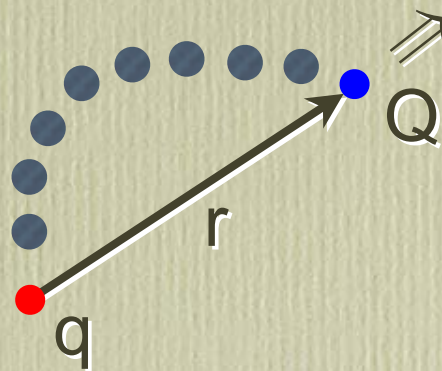
$$C(LM_L(SM_S; \Lambda\{n_{\alpha_1}, n_{\alpha_2}\})) = (-1)^{k+s+\Lambda+N} LM_L(SM_S; \Lambda\{n_{\alpha_1}, n_{\alpha_2}\})$$

$\Lambda + \zeta$  ( $-\Lambda$ )

# Adiabatic Surface Quantum Numbers

the diatomic molecule

$\Lambda = \Sigma, \Pi, \Delta, \dots$

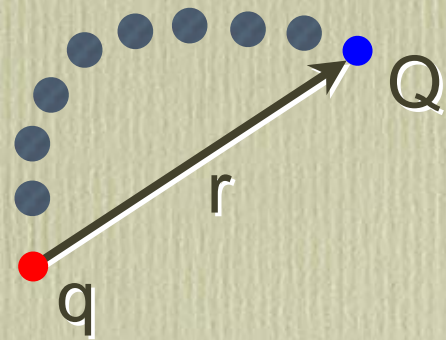


projection of the string angular momentum  
onto the  $qq$  axis

# Adiabatic Surface Quantum Numbers

the diatomic molecule

$$\eta = u/g$$

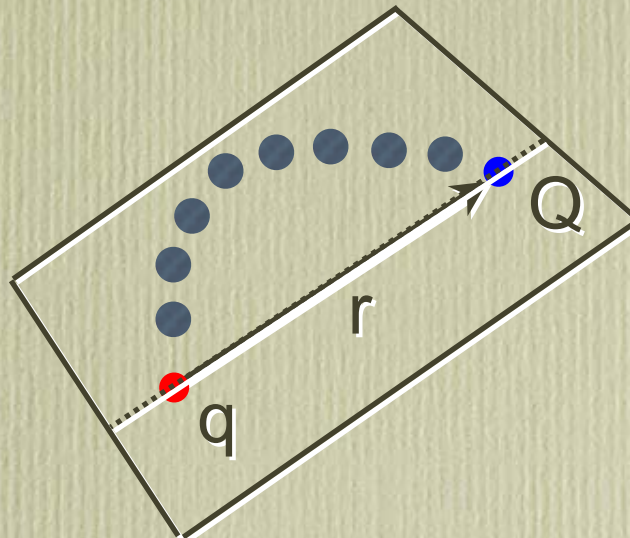


PC acting on the glue

# Adiabatic Surface Quantum Numbers

the diatomic molecule

$Y = +/ -$



reflection in a plane containing the  $q\bar{q}$  axis

ex:  $\Lambda_\eta^Y = \sum_g \frac{+}{-}$  ground state

# Hybrid Quantum Numbers (one m=1 phonon)

L	S	J <sup>PC</sup>
1	0	1++
1	1	(2,1,0) <sup>+ -</sup>
2	0	2--
2	1	(3,2,1) <sup>+ +</sup>
$\zeta = +$	1	1--
	1	(2,1,0) <sup>+ +</sup>
	2	2++
	2	(3,2,1) <sup>+ -</sup>
$\zeta = -$	1	1--
	1	(2,1,0) <sup>+ +</sup>
	2	2++
	2	(3,2,1) <sup>+ -</sup>

# FTM Model Hamiltonian

$$H_{FTM} = \frac{1}{2\mu} \frac{\partial^2}{\partial r^2} - L(L-1) \frac{\lambda^2}{2\mu r^2} + \cancel{(L^2)} + \frac{4\alpha_s}{3c} \delta_r - \frac{\pi}{r} (1 - c^{-1} \sqrt{L})$$

## I&P Hybrid Masses

flavour	$m$	$m'$
$ =1$	1.67	1.9
$ =0$	1.67	1.9
$s\bar{s}$	1.91	2.1
$c\bar{c}$	4.19	4.3
$b\bar{b}$	10.79	10.8

2  $\begin{smallmatrix} +,1 \\ -,1 \end{smallmatrix}$   $\begin{smallmatrix} +,0 \\ -,0 \end{smallmatrix}$   $\begin{smallmatrix} +,1 \\ -,1 \end{smallmatrix}$   $\begin{smallmatrix} ++ \\ -- \end{smallmatrix}$

Aside:

Giles and Tye, PRL37, 1175  
(1976)

Coupled quarks to a relativistic 2d sheet... the “Quark Confining String Model”.

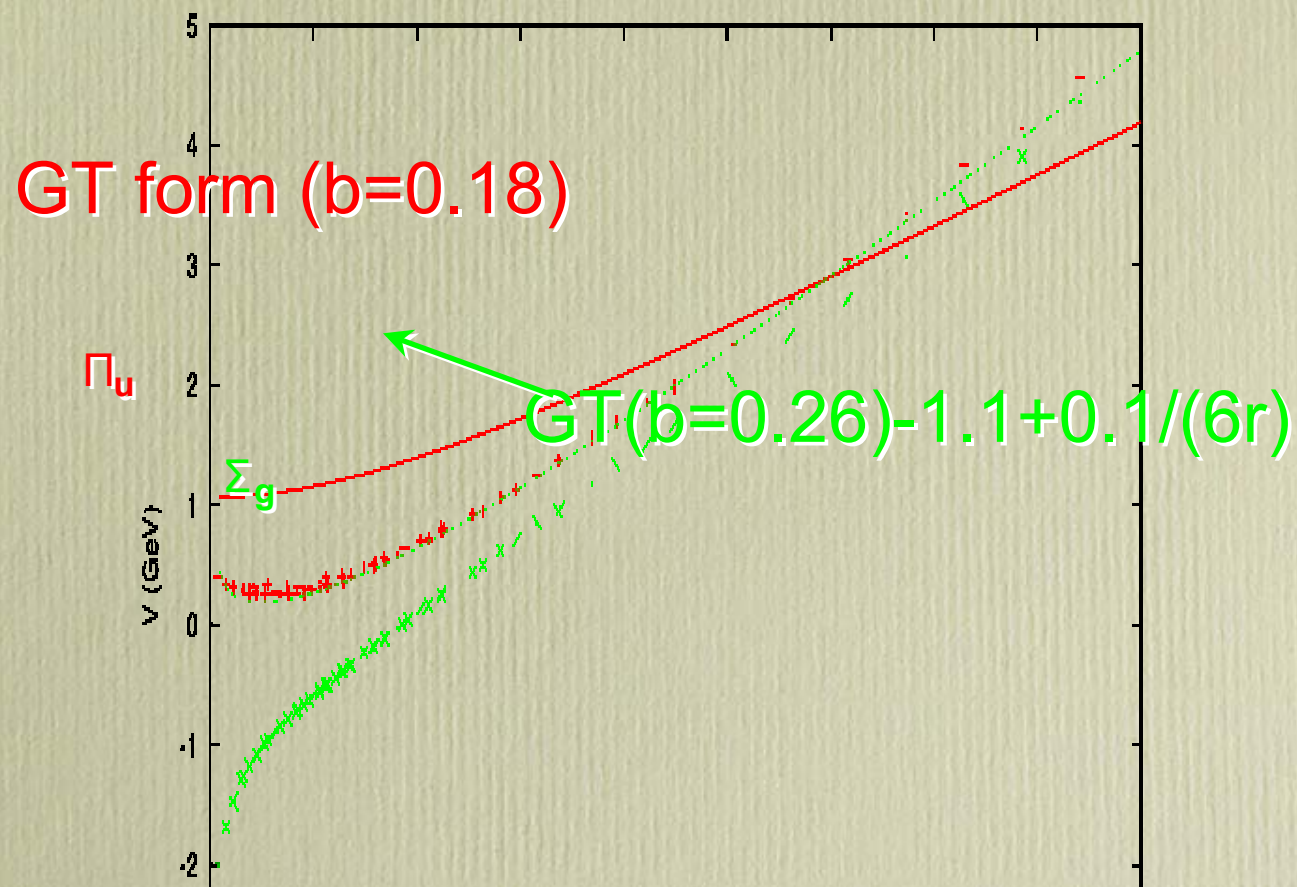
“The presence of vibrational levels gives ... extra states in quantum mechanics. ... that are absent in the charmonium model.”

$$V_N = \sigma r \left(1 + \frac{2N\pi}{r^2}\right)^{-1/2}$$

GT

$$V_{NG} = \sigma r \left(1 - \frac{R^2}{r^2} + \frac{2N\pi}{r^2}\right)^{-1/2}$$

J.F. Arvis, PLB127, 106 (83); Luescher



GT also  
computed finite-  
mass  
corrections, and  
spin-orbit  
splittings.

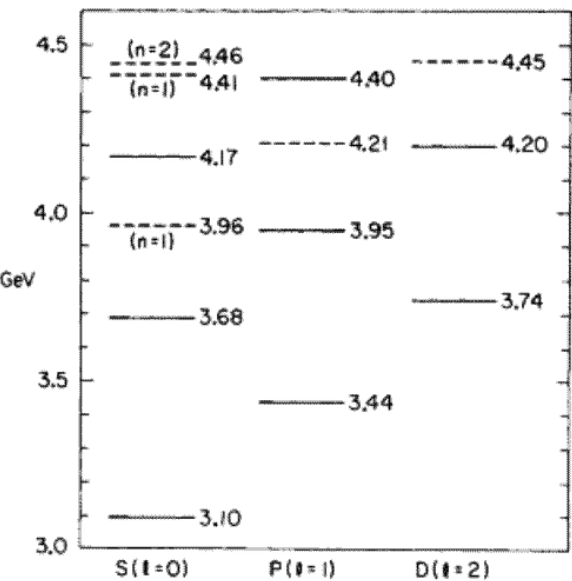
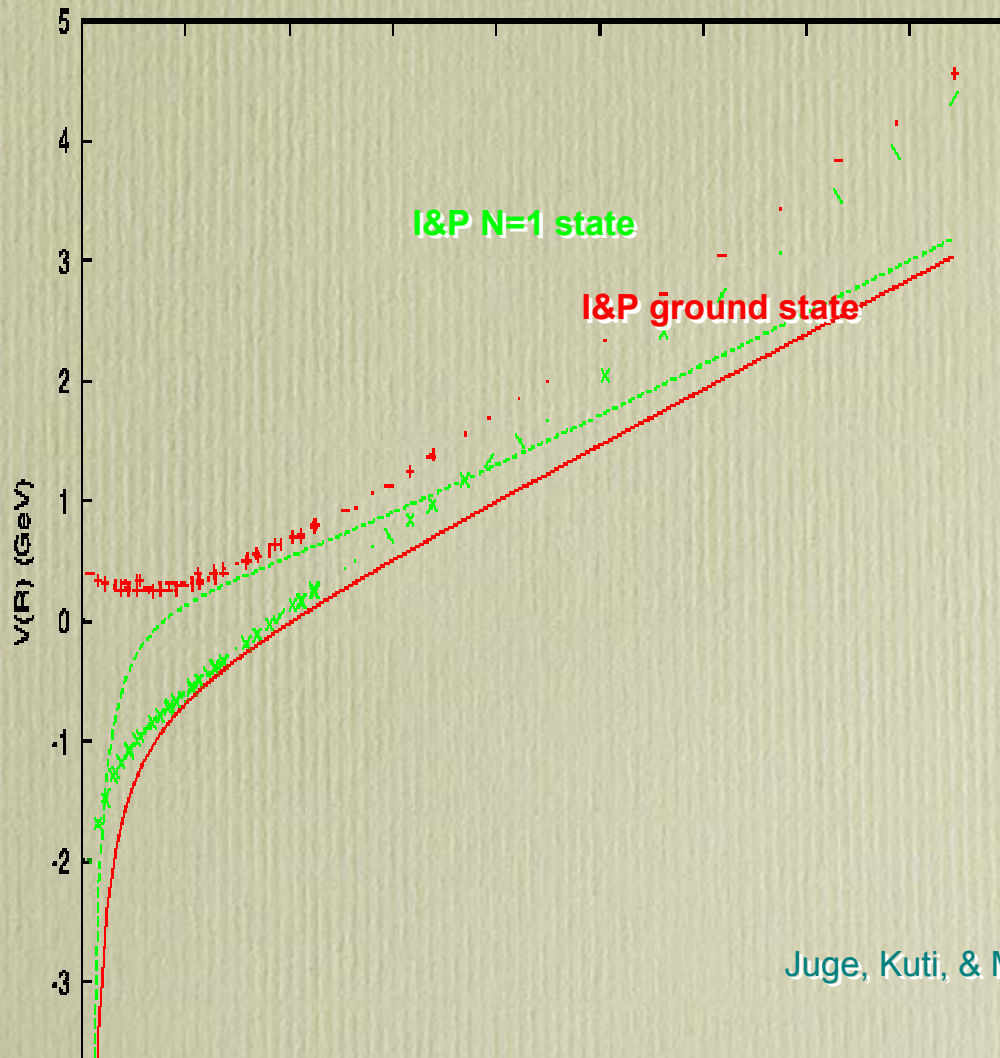


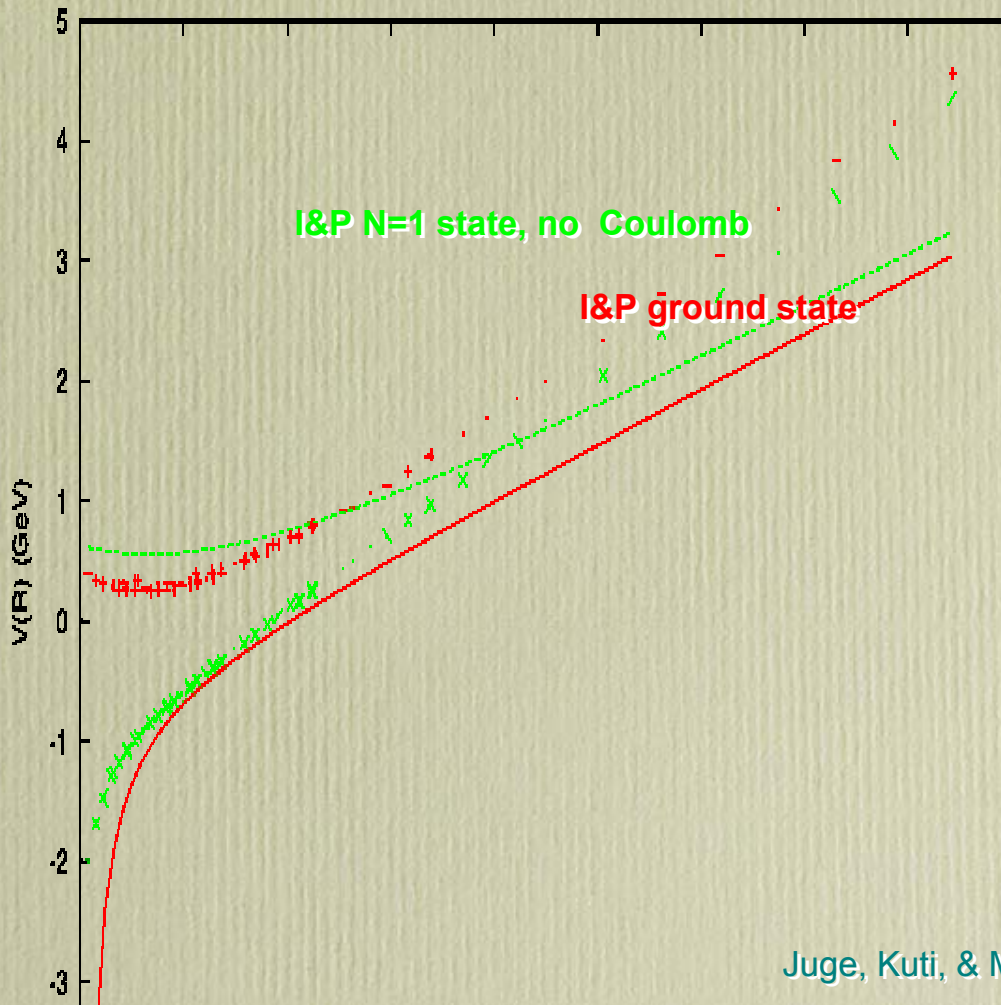
FIG. 4. The nonrelativistic spectroscopy of the charm string.  $\psi(3.10)$  and  $\psi(3.68)$  are fitted to obtain  $M = 1.154$  GeV and  $k = 0.21$  GeV $^2$ . The dashed lines are the vibrational levels absent in the charmonium model. Levels with  $E > 4.5$  GeV or  $l > 2$  are not shown.

# Checks

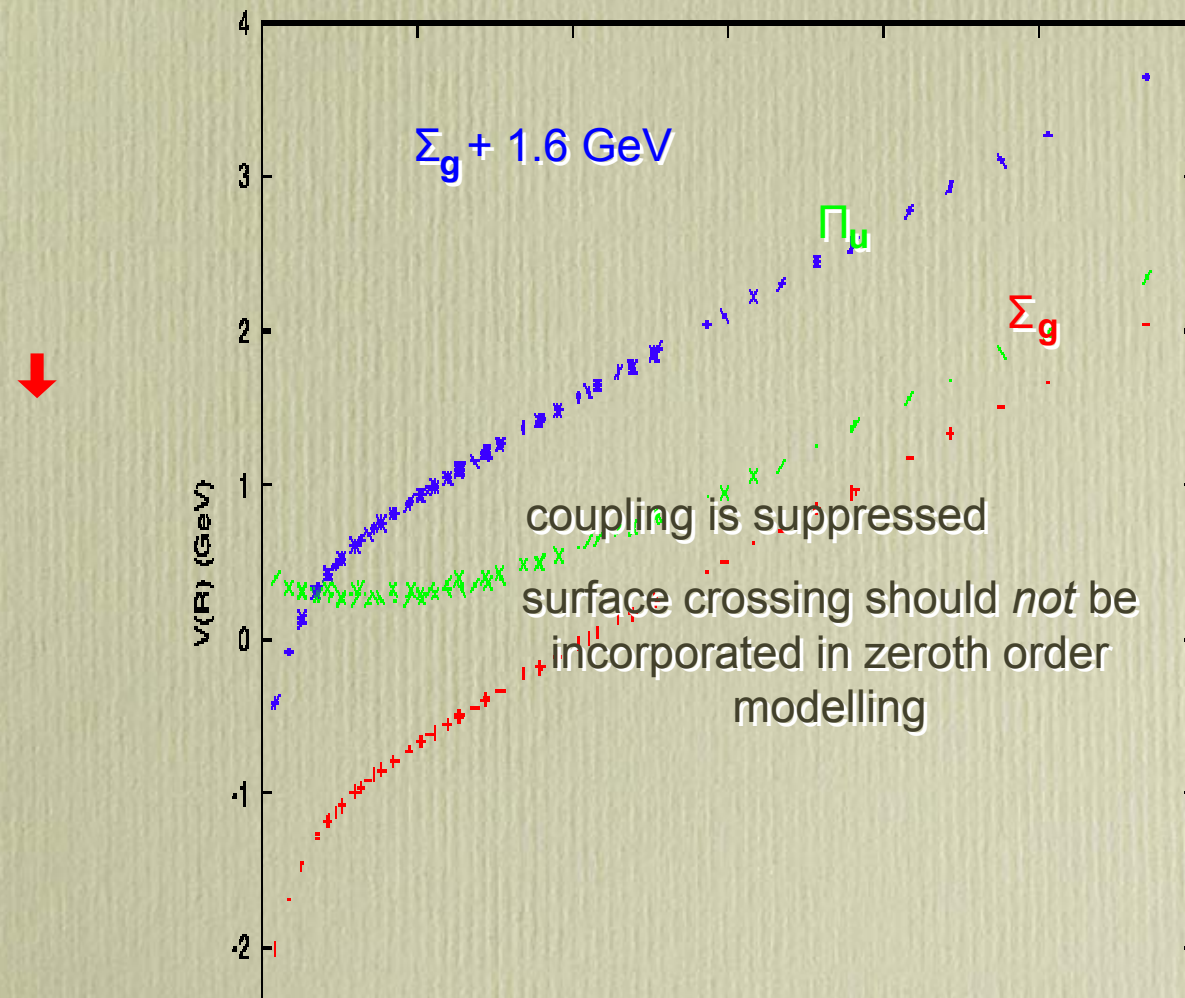
# Comparison to the lattice



# Comparison to the lattice



# Should the Coulomb potential be there?

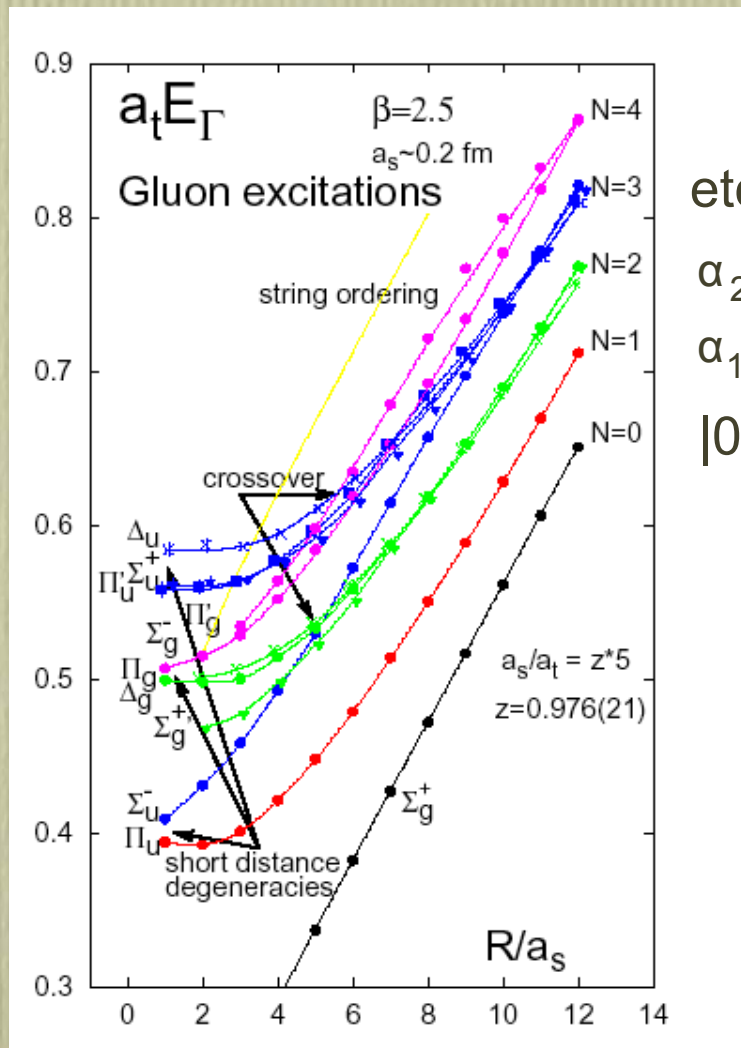


# Born-Oppenheimer + lattice potentials

$$H_{\text{tot}} = \frac{1}{2m} \frac{\partial^2}{\partial r^2} + \frac{L(L+1) - 2\lambda^2 + i\gamma_4}{2m} + V_L$$

flavour	m	m'	lat
=1	1.67	1.9	1.85
=0	1.67	1.9	1.85
s̄s̄	1.91	2.1	2.07
c̄c̄	4.19	4.3	4.34
b̄b̄	10.79	10.8	10.85

# strings and flux tubes

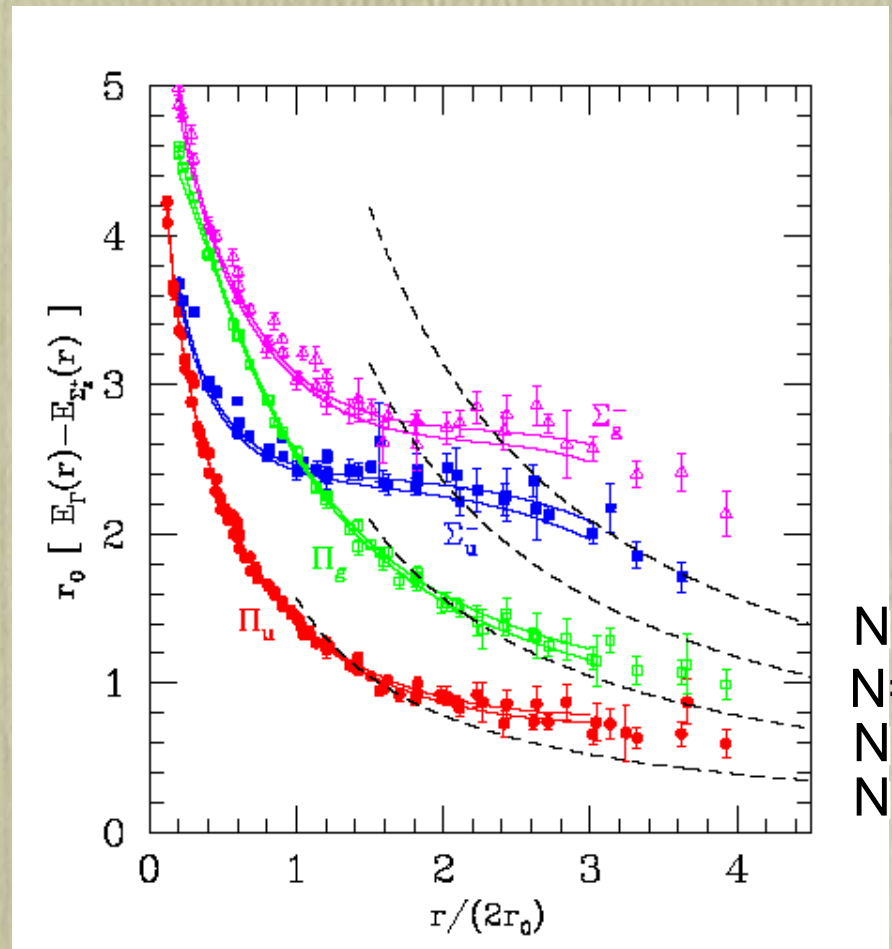


etc

$\alpha_{2+}^\square |0\rangle \alpha_{2-}^\square |0\rangle;$   
 $\alpha_{1+}^\square \alpha_{1+}^\square |0\rangle \alpha_{1-}^\square \alpha_{1-}^\square |0\rangle,$   
 $\alpha_{1+}^\square \alpha_{1-}^\square |0\rangle$

|0>

# strings and flux tubes



# Adiabatic and small oscillation approximations

Barnes, Close, & ES, PRD52, 5242 (95)

$$H_{\text{full}} = \frac{1}{2m_b} \sum_{i=1}^N \left( \sum_{j,r} i_{ijr} (\vec{\nabla}_i)^2 \right) + \sum_{i=1}^{N-1} V(r_i) + \frac{E(R)}{E_0(R)}$$

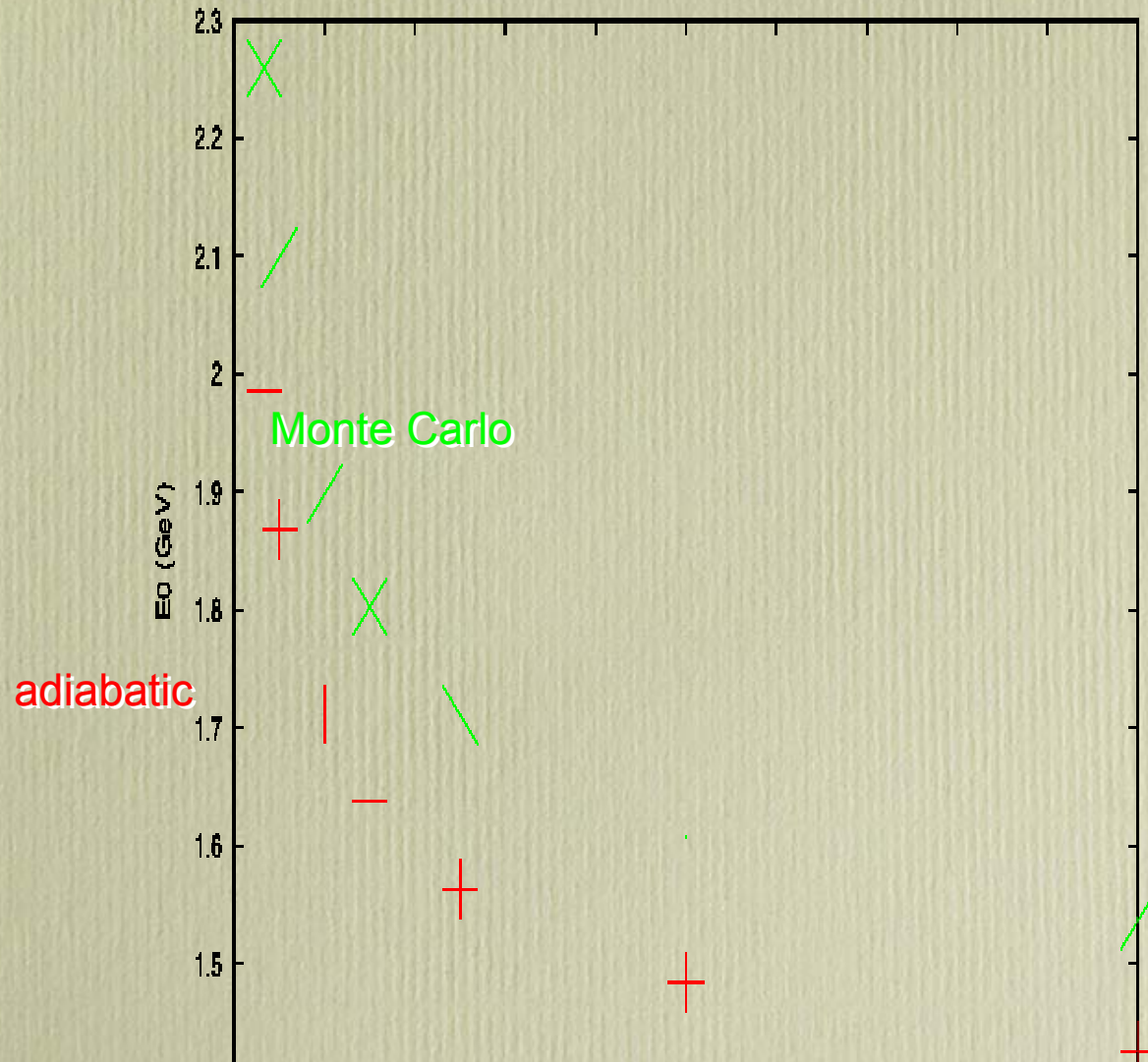
$m_b = 0.2 \text{ GeV}$   
 linear potential

Adiabatic limit (check small  
osc)



Fig.1. Ground state and first hybrid adiabatic potentials and their difference, for  $N=2$ .  
 Solid lines are exact and dashed lines are the small oscillation approximation.  
 String tension  $a=1.0 \text{ GeV/fm}$ , bead mass  $m_b=0.2 \text{ GeV}$ .

## Adiabatic approximation (ground state meson)



## Adiabatic approximation (hybrid gap)

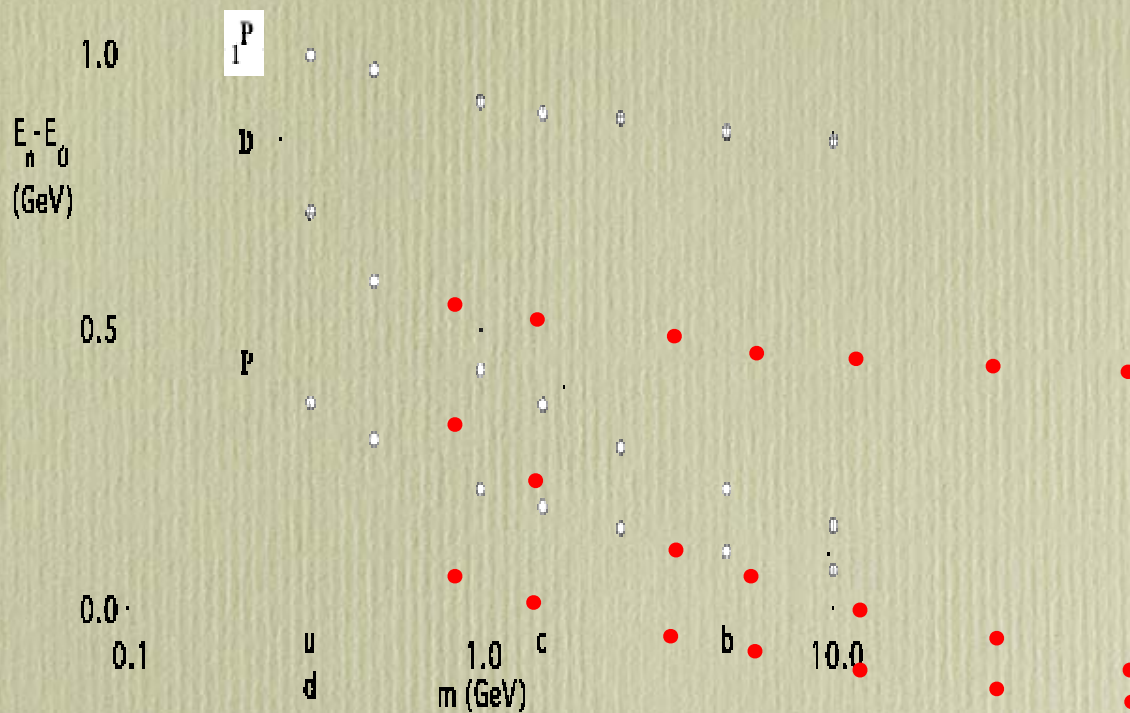


Fig.4. Energies of the lightest  $L=1,2$   $\bar{q}q$  and  $L=P$  hybrid states relative to  $E_0 = E_s$  for  $N=1$ . Lines show the adiabatic approximation and the points are Monte Carlo,  $M=0$  (open) and  $M=L$  (plus);  $b=0.2\text{ GeV}$ ,  $a=1.0\text{ GeV/fm}$ ,  $\alpha_s=0$ .

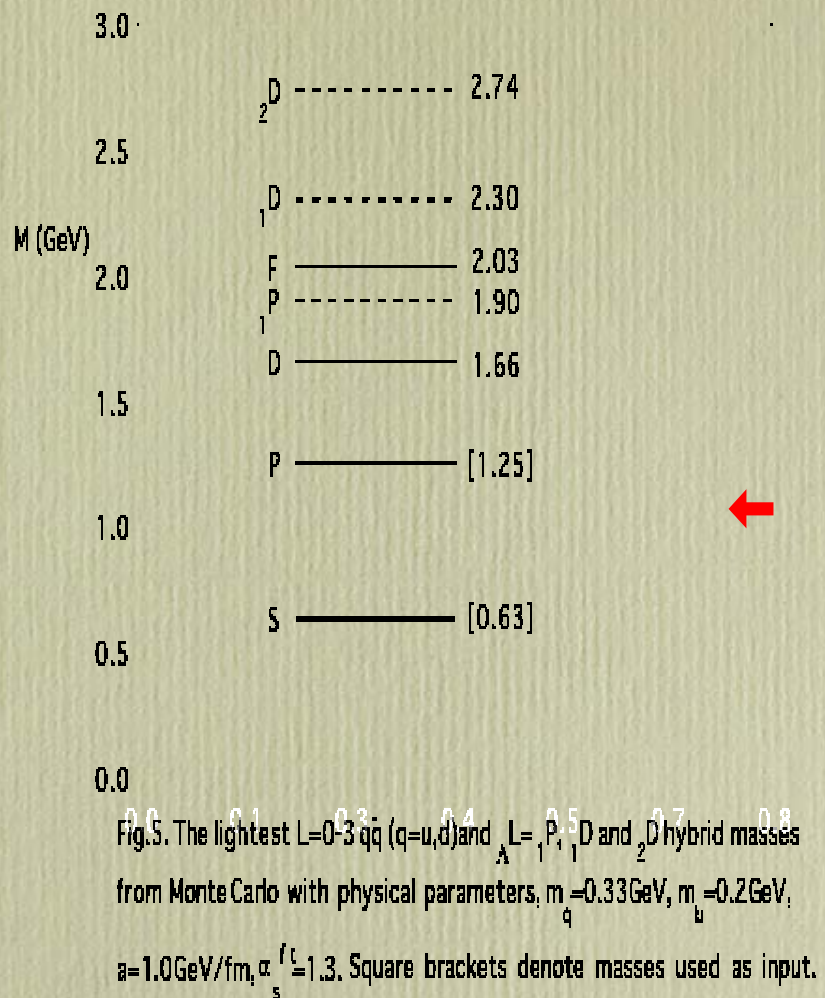


Fig.5. The lightest  $L=0,3$   $q\bar{q}$  ( $q=u,d$ ) and  $L=1,2,5$   $D$  and  $D_s$  hybrid masses  
 from Monte Carlo with physical parameters,  $m_u = 0.33$  GeV,  $m_d = 0.2$  GeV,

$a = 1.0$  GeV/fm,  $\alpha_s^{fitter} = 1.3$ . Square brackets denote masses used as input.

# IKP decay model

# quark creation operator

$$H = \frac{g^2}{2a} \sum_i E_i^\dagger E_{i\mu} + \sum_n m_n c_n c_{n\mu} + \frac{1}{a} \sum_n (\psi_n^\dagger \alpha_n U_\mu(n) c_{n+\mu} + \frac{1}{4a^2} \sum_p (\beta(N - U_p - U_p^*)$$

↓

$$H_{int} \sim \psi_n^\dagger \alpha_n \mu c_{n+\mu}$$

$$\sim \psi_n^\dagger \alpha_n \mu c_{n+\mu} - \alpha_n^\dagger \psi_n \mu \nabla c_{n+\mu}$$



$$\psi_n^\dagger \alpha_n \mu c_{n+\mu} \quad \psi_n^\dagger \alpha_n \nabla c_{n+\mu}$$

$^3S_1$

$^3P_0$

# flux tube overlaps

Kokoski & Isgur, PRD35, 907 (87)

meson decay

$$\langle \{0\dots 0\} bd; \{0\dots 0\} bd | O | \{0\dots 0\} bd \rangle \sim \langle bd; bd | {}^3P_0 | bd \rangle .$$

$$\langle \{0\dots 0\}; \{0\dots 0\} | \{0\dots 0\} \rangle$$



hybrid decay

Isgur, Kokoski, & Paton, PRL54, 869 (85)

$$\langle \{0\dots 0\} bd; \{0\dots 0\} bd | O | \{1,0\dots 0\} bd \rangle \sim \langle bd; bd | {}^3P_0 | bd \rangle .$$

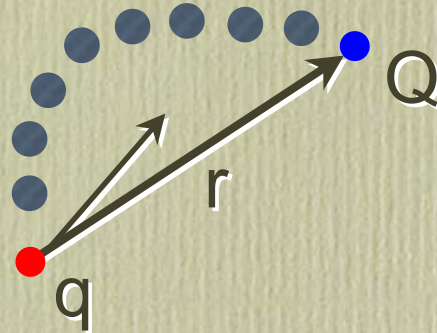
$$\langle \{0\dots 0\}; \{0\dots 0\} | \{1,0\dots 0\} \rangle$$

$$y_\perp e^{-f b} y_\perp^2$$

# Extensions

## A. Charge Radii

Isgur, PRD60,114016 (99)



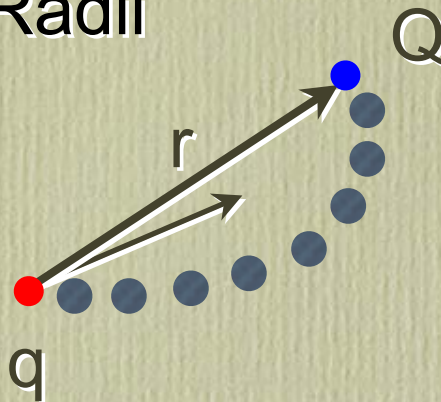
flux tube zero point motion induces transverse oscillation in the quarks → larger charge radius

$$r_0^2 = \left( \frac{m_q}{\omega_{z0} + m_q} \right)^2 + \frac{\delta_{\text{osc}}^2(3)}{\omega_{z0}^2} \langle r^2 \rangle$$

increased elastic form factor slope → flux lost to hybrid production

## A. Charge Radii

Isgur, PRD60,114016 (99)



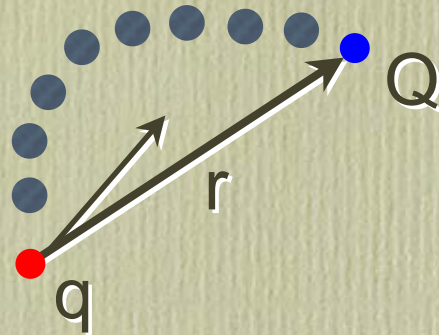
flux tube zero point motion induces transverse oscillation in the quarks → larger charge radius

$$r_Q^2 = \left( \frac{m_Q}{m_q + m_g} \right)^2 \cdot \frac{\delta_{\text{osc}}^2(3)}{\pi^2 g_s^2} \langle r^2 \rangle$$

increased elastic form factor slope → flux lost to hybrid production

## A. Charge Radii

Isgur, PRD60,114016 (99)



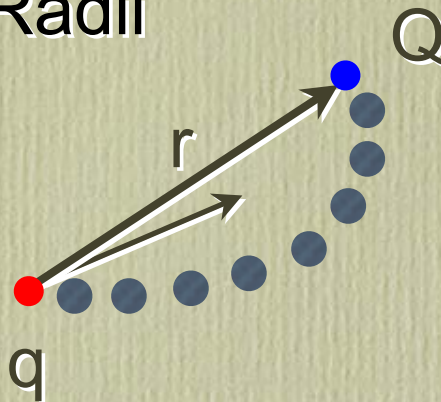
flux tube zero point motion induces transverse oscillation in the quarks → larger charge radius

$$r_0^2 = \left( \frac{m_q}{\omega_{z0} + m_q} \right)^2 + \frac{\delta_{\text{osc}}^2(3)}{\omega_{z0}^2} \langle r^2 \rangle$$

increased elastic form factor slope → flux lost to hybrid production

## A. Charge Radii

Isgur, PRD60,114016 (99)



flux tube zero point motion induces transverse oscillation in the quarks → larger charge radius

$$r_Q^2 = \left| \left( \frac{m_Q}{m_{\text{sum}}} \right)^2 + \frac{\delta_{\text{sum}}^2}{m_{\text{sum}}} \langle \bar{s} s \rangle \langle r^2 \rangle \right|$$

increased elastic form factor slope → flux lost to hybrid production

## B. Adiabatic Surface Mixing

Merlin & Paton, J. Phys. G11, 439 (85)

adiabatic surface mixing is induced by terms neglected by I&P, eg:

$$H_1 = \frac{1}{2m\pi^2} \left( L_{xx}^2 - L_{yy}^2 - 2L_{xy}L_{yx} - 2L_x L_{yyx} \right)$$

resulting mass shifts were quoted in I&P

# C. Spin-Orbit Force

Merlin & Paton, PRD35, 1668 (87)

$$H' = \frac{e}{2m} \boldsymbol{\sigma} \cdot \boldsymbol{B} = T^a B^a(r) \sim \frac{1}{2r_{eff}} \frac{T^a(r_{eff})}{r_{eff}}$$

obtain a small spin-orbit shift and conclude that  
spin-orbit splittings are mostly due to Thomas precession

$$H_{TS} = \frac{1}{4} (\vec{r}_n \times \vec{v}_n) \cdot \boldsymbol{\sigma}$$

$$\vec{v}_n = \frac{1}{2} \times \frac{2\pi}{\omega_n + 2\omega_{ex}} \sum_{l=1}^{\infty} (-1)^{l+1} \frac{(2l+1)\omega_l}{(\omega_n + 2\omega_{ex})^{l+1}} \vec{e}_{nl}$$

find sing splittings of: -140 (2+-) -20 (2-+) 20 (1-+) 40 (0-+)  
140 (1+-) 280 (0+-) 0 (1++) 0 (1--)

# D. Spin-Orbit Force, II

Szczepaniak & ES, PRD55, 3987 (97)

map chromofields to phonon degrees of freedom

$$E_N^X(n) = \frac{2\pi}{L} (\eta_X^N(n+1) - \eta_X^N(n))$$

$$B_N^X(n) = \frac{1}{n!} \frac{\partial^n}{\partial \eta_X^N(n)}$$

$$N = n_V k_0$$

$$B_N^X(n) = \frac{1}{n!} \sqrt{\frac{2\pi}{\lambda}} \sum_{\omega_m} \sin \frac{\pi m}{N+1} n \sqrt{\omega_m} \left( \alpha_{m,\lambda}^{(N)} e^{-\omega_m t} - \alpha_{m,\lambda}^{(N)} e^{\omega_m t} \right)$$

# spin-dependence in the confinement potential

$$V_{conf} \rightarrow \epsilon + V_{SD} + \dots$$

$\Gamma$	$\epsilon_\Gamma$	$V_1$	$V_2$	$V_3$	$V_4$
scalar	$S$	$-S$	0	0	0
vector	$V$	0	$V$	$V'/r - V''$	$2\nabla^2 V$
pseudoscalar	0	0	0	$P'' - P'/r$	$\nabla^2 P$

Gromes

$$\begin{aligned} V_{SD} = & \left( \frac{\sigma_q \cdot L_q}{4m_q^2} - \frac{\sigma_{\bar{q}} \cdot L_{\bar{q}}}{4m_{\bar{q}}^2} \right) \left( \frac{1}{r} \frac{d\epsilon}{r} + \frac{2}{r} \frac{dV_1}{dr} \right) + \left( \frac{\sigma_q \cdot L_q}{2m_a m_q} - \frac{\sigma_{\bar{q}} \cdot L_{\bar{q}}}{2m_{\bar{q}} m_q} \right) \left( \frac{1}{r} \frac{dV_2}{dr} \right) \\ & + \frac{1}{12m_q m_{\bar{q}}} (3\sigma_q \cdot \hat{r} \sigma_{\bar{q}} \cdot \hat{r} - \sigma_q \cdot \sigma_{\bar{q}}) V_3(r) + \frac{1}{12m_q m_{\bar{q}}} \sigma_q \cdot \sigma_{\bar{q}} V_4(r) \end{aligned}$$

Eichten & Feinberg  
Ng, Pantaleone, & Tye

# spin-dependence in the confinement potential

examine in Coulomb gauge via the Foldy-Wouthuysen transformation

$$H_{QCD} \rightarrow H_{FW} = \int dx \left( m_q h^\dagger(x) h(x) - m_{\bar{q}} \chi^\dagger(x) \chi(x) \right) + H_{YM} + \\ + V_C + H_1 + H_2 + \dots$$

$$H_1 = \frac{1}{2m_q} \int dx h^\dagger(x) \left( D^2 - g\sigma \cdot B \right) h(x) - (h \rightarrow \chi; m_q \rightarrow m_{\bar{q}})$$

$$H_2 = \frac{1}{8m_q^2} \int dx h^\dagger(x) g\sigma \cdot [E, \times D] h(x) - (h \rightarrow \chi; m_q \rightarrow m_{\bar{q}})$$

$$D = i\nabla + gA$$

$$E^a = -\Pi^a + E_\ell^a$$

$$E_\ell^a = -\nabla A_0^a - g\nabla\nabla^{-2}f^{abc}A^b \cdot \nabla A_0^c$$

$$A_0^a(x) = g \int dy V^{ab}(x, y; A) \rho^b(y)$$

# spin-dependence in the confinement potential

perform Rayleigh-Schrödinger perturbation theory

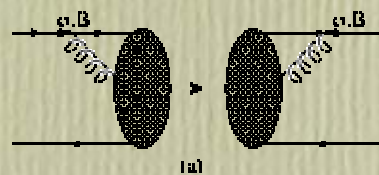
basis:  $H_0|n_r; r_q r_{\bar{q}}\rangle = \epsilon_n(r)|n_r; r_q r_{\bar{q}}\rangle$

first order:  $\delta\epsilon_n^{(1)}(r) = \langle n_r; r_q r_{\bar{q}} | H_2 | n_r; r_q r_{\bar{q}} \rangle$

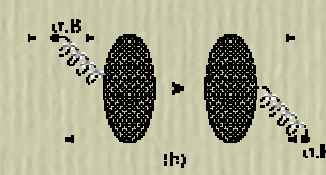
$$\langle n_r | \nabla_{r_q}^j g^2 T^a V^{ab}(r_q, r_{\bar{q}}; A) T^b | n_r \rangle = -\nabla_{r_q}^j \epsilon_n(r)$$

$$\delta\epsilon_n^{(1)} = \left( \frac{\sigma_q \cdot L_q}{4m_q^2} - \frac{\sigma_{\bar{q}} \cdot L_{\bar{q}}}{4m_{\bar{q}}^2} \right) \frac{1}{r} \frac{d\epsilon_n}{dr}$$

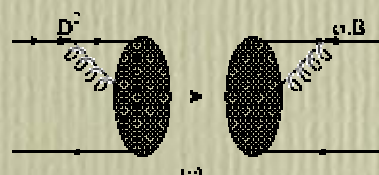
## second order perturbation theory in $H$



zero



hyperfine + tensor



$V_1$



$V_2$

evaluate matrix elements in the flux tube model:

$$V_1 = \sigma r; \quad V_2 = O(1/N)$$

# E. Vector Decay Model

use the same mapping to obtain  $\bar{\psi} \alpha \cdot A \psi$

$$H_{int} = \frac{m^2}{\sqrt{\pi}} \sum_{n,m,\lambda} \int_0^1 d\zeta \cos(\pi\zeta) T_{\ell,n}^{(1)}(\theta) (\zeta r_{\ell,n})^\sigma e_\lambda(r_{\ell,n}) \left( \alpha_{m\lambda}^{(1)} - \alpha_{m\lambda}^{(2)} \right) \chi_\ell(\zeta r_{\ell,n})$$

$$\langle H | H_{int} | MR \rangle = \left( \frac{m^2}{\pi} \right)^{\frac{1}{2}} \int_0^1 d\zeta \int dx \cos(\pi\zeta) \sqrt{\frac{2k_m+1}{15}} e^{\frac{-2k_m}{15}x^2} \epsilon_R(x) \epsilon_L^\dagger(\zeta r) \epsilon_L^\dagger(x) (1 - \zeta(x)) \right. \\ \left. \left[ D_{M,\lambda}^{(1,n)}(x, \theta, -r) \chi_{\ell,\lambda}^{(1)} e_\lambda(r) - \langle \sigma \rangle \right] \right]$$

## F. Other

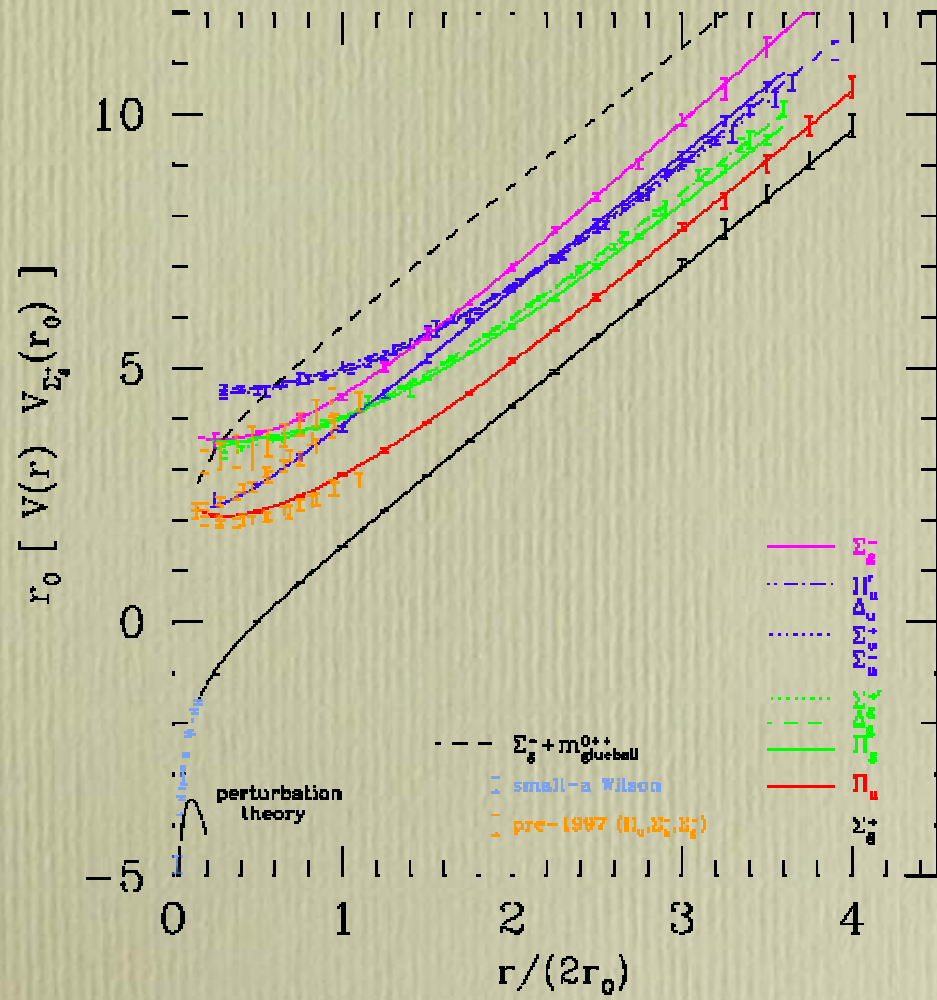
- glueballs (glue loops)
- baryons
- check Luescher term and adiabatic surfaces
- apply to glueloops in SU(2)
- apply to 2+1 U(1)
- improve semiclassical fragmentation formalism
- examine long range spin-spin and spin-orbit forces

# Conclusions

- ➊ the FTM provides a compelling picture of strong QCD dynamics
- ➋ it is a picture only!
- ➌ many extensions and applications, explored and unexplored, exist

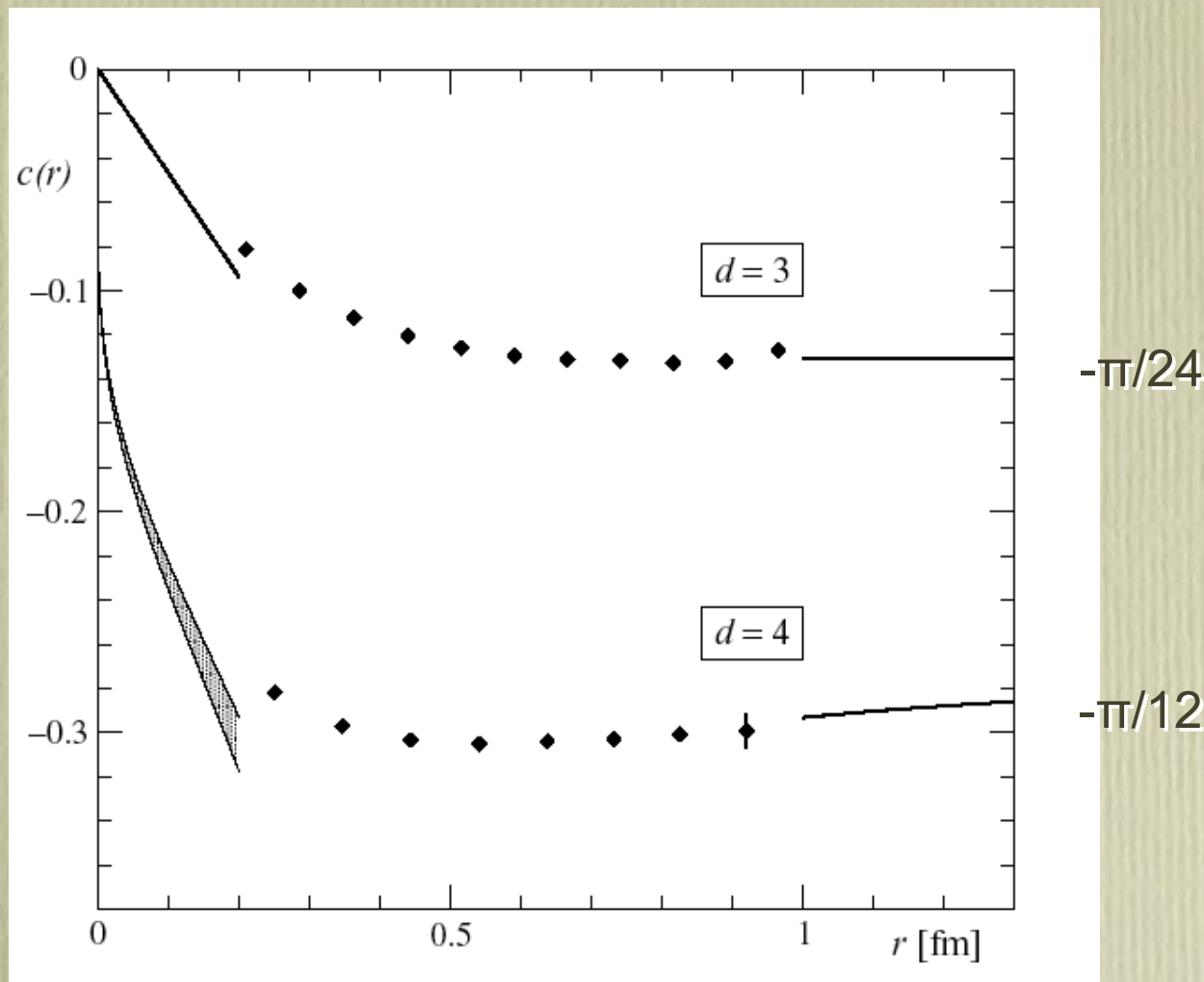
***fin***

# strings and flux tubes



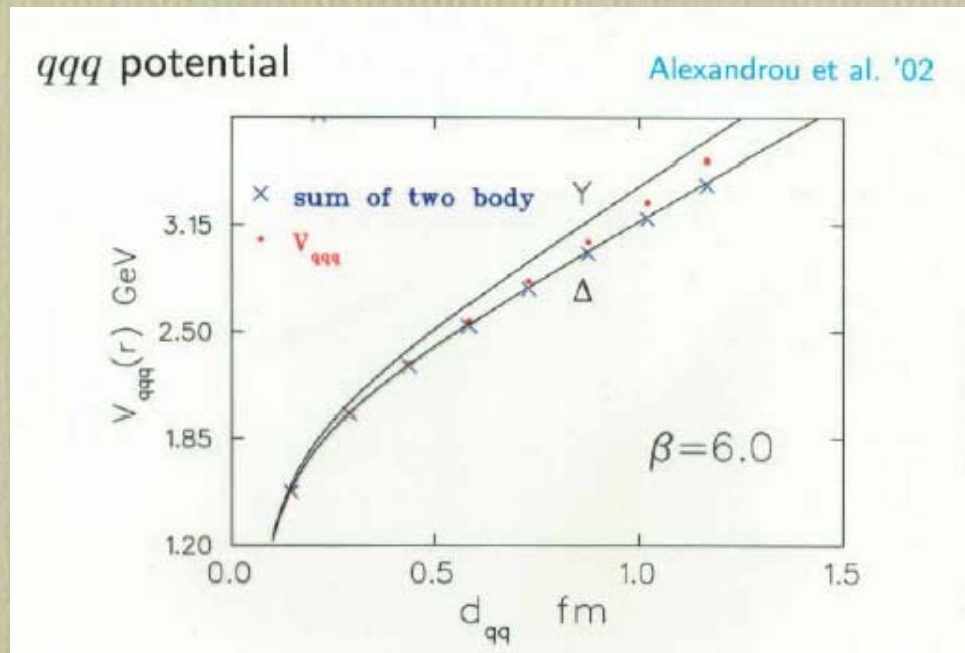
# strings and flux tubes

Lüscher & Weisz

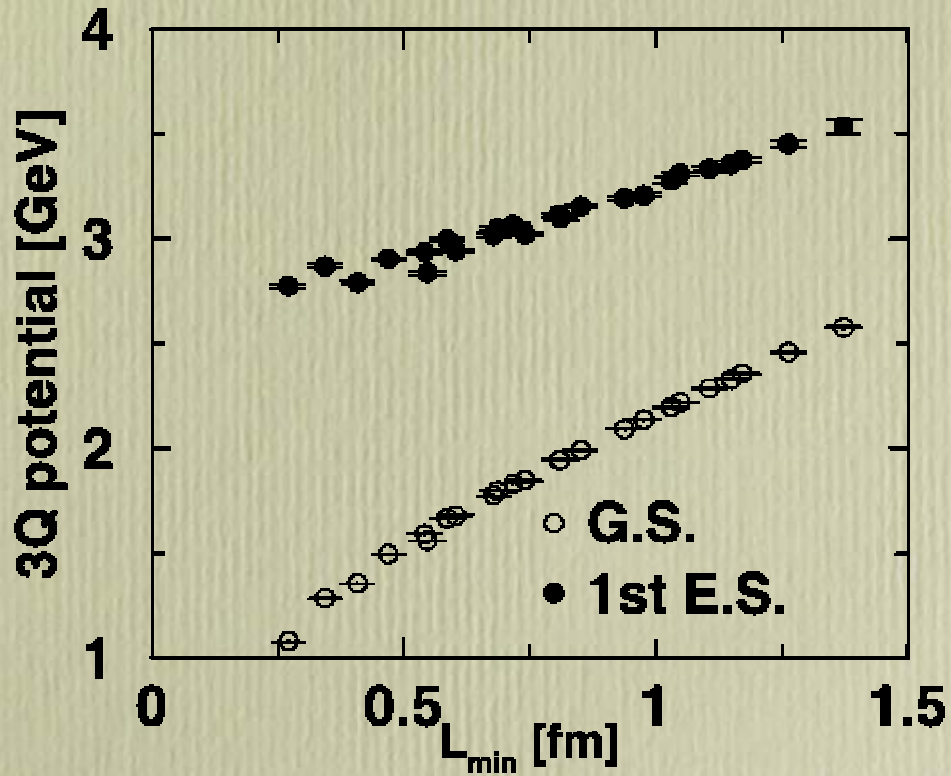


see talk by Juge

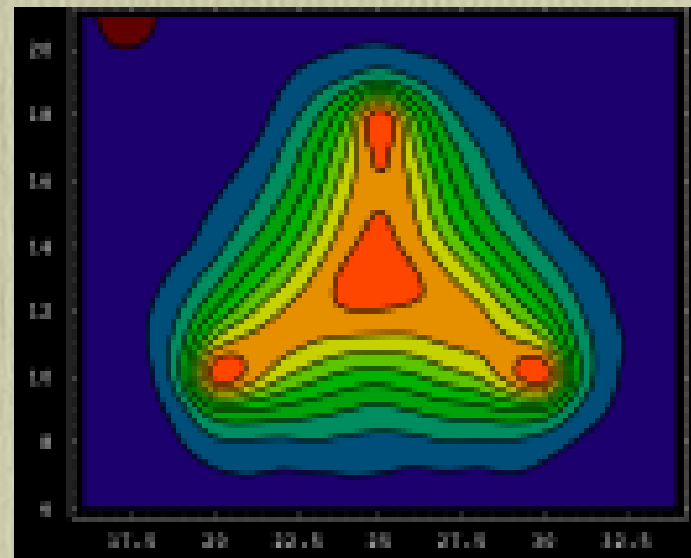
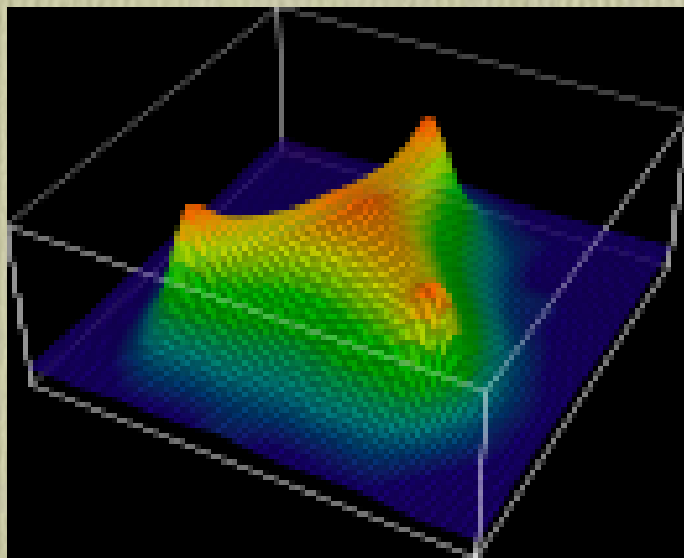
# strings and flux tubes



# strings and flux tubes



# strings and flux tubes



Ichie, Bornyakov, Schierholz, & Streuer, hep-lat/0212036

# strings and flux tubes

